Geological control on carbon isotope equilibrium and kinetic fractionation of CH_4-CO_2-HCO_3^- in microbial coalbed and shale gas systems

Xiangrui Chen[1,2], Mingxin Tao[2,*], Zheng Zhou[3], Greg Holland[4], Yunpeng Wang[1,*]

[1]*State Key Laboratory of Organic Geochemistry, Guangzhou Institute of Geochemistry, Chinese Academy of Sciences, 510640, China*

[2]*Faculty of Geographical Science, Beijing Normal University, 100875, China*

[3]*Lancaster Environment Centre, Lancaster University, LA1 4YQ, UK*

[4]*Department of Earth and Environmental Sciences, The University of Manchester, M13 9PL, UK*

*Corresponding author. Email: mxtao@bnu.edu.cn; wangyp@gig.ac.cn

Abstract

Microbial coalbed gas (CBG) and shale gas (SG), predominately composed of methane (CH_4) and carbon dioxide (CO_2), are important economic resources and potent greenhouse gases. Although isotopic equilibrium of CH_4 and CO_2 has been observed in microbial CBG and SG basins, it is difficult to judge under what geological conditions equilibrium is achieved. Moreover, the effects of CO_2 dissolution on the isotopic fractionation process need to be

considered. We use data from eight microbial CBG and SG basins to discuss the geological conditions in which equilibrium and kinetic isotopic fractionation in CH_4-CO_2-HCO_3^- system is achieved. Based on isotopic equilibrium temperatures calculated using computer codes developed in MatLab software, we show that, in deep and closed reservoirs, the CH_4-CO_2 and CH_4-HCO_3^- are close to carbon isotope equilibrium. In contrast, in shallow and open reservoirs, they are in disequilibrium. The CO_2-HCO_3^- is in disequilibrium in most reservoirs. We propose that both low free energy gradients and long coexisting time of CH_4 and CO_2/HCO_3^- are necessary to attain isotopic equilibrium. However, it is difficult to accurately estimate the timescale for attaining isotope equilibrium among them. In general, a closed and deep CBG/SG reservoir is likely to be geologically and geochemically stable over long timescales, favoring isotopic equilibrium of CH_4-CO_2 and CH_4-HCO_3^-. However, a shallow and open reservoir is unfavourable for their isotopic equilibrium due to shorter timescales for the coexistence of CH_4-CO_2-HCO_3^-. Using data from systems close to equilibrium, we estimated the percentage of CO_2 in total CH_4 and CO_2 in CBG reservoirs in various basins to be from 27% to 50%, where methanogenesis is mainly by CO_2 reduction. This is significantly higher than the CO_2 content (1% to 15%) in gaseous CH_4 and CO_2 in these basins but is consistent with those (36% to 48%) from culture experiments for coal conversion by methanogenesis. Further study shows that 53-99% of the CO_2 formed during CBG generation has dissolved into groundwaters to form dissolved inorganic carbon (DIC) in CBG reservoirs. We propose that CO_2 dissolution likely has significantly affect the abundance and isotopic compositions of gaseous CO_2 in subsurface.

Keywords: Microbial gas; Carbon isotope; equilibrium or kinetic fractionation; CO_2 dissolution; CO_2/CH_4

1. Introduction

Microbial natural gas, whose predominate components are methane (CH_4) and carbon dioxide (CO_2), is an important economic resource and a potent greenhouse gas. Isotopic compositions of CH_4 and CO_2 can record the formation and evolution processes of microbial natural gas (Whiticar et al., 1986; Milkov and Etiope, 2018). Although there is an ongoing debate concerning the relative importance of kinetic and equilibrium processes in controlling isotopic compositions and distributions of microbial natural gas, it is often assumed that kinetic processes are dominant (Whiticar et al., 1986; Gropp et al., 2021; Turner et al., 2021). By comparing isotopic fractionation factors $\alpha_{CO2\text{-}CH4}$ of microbial gas samples from natural environments and culture experiments with those expected for equilibrium based on the environmental temperatures, Whiticar et al. (1986) suggested that kinetic processes largely control the isotopic compositions of microbial CH_4 and CO_2. They proposed that many processes such as, slow isotope exchange rate, rapid methanogenesis rate, admixture of methane with different origins, and methane oxidation cause kinetic isotopic fractionation of CH_4 and CO_2. Based on isotopic kinetic effects $\delta^{13}C_{CH4}$, $\delta^{13}C_{CH4}$ vs. δD_{CH4}, $\delta^{13}C_{CH4}$ vs. $\delta^{13}C_{CO2}$, δD_{CH4} vs. δD_{H2O} have been used frequently for tracing origins, migrations, and formation pathways of microbial natural gas (Whiticar, 1999; Golding et al., 2013; Milkov and Etiope, 2018).

Isotopic equilibrium is also observed in microbial natural gas systems. Smith et al. (1981) proposed that microbial CH_4 approaches carbon isotopic equilibrium with CO_2 in Australian CBG. Meister et al. (2019) found that the microbial CH_4 and CO_2 from deep marine sediments are close to carbon isotopic equilibrium. They proposed that methanogenic microbial organisms catalyzed CH_4-CO_2 isotopic equilibration. Turner et al. (2021) compiled an isotopic dataset

(n >800) of microbial CH_4 and co-occurring CO_2 and H_2O from various environments. By comparing the differences between measured and calculated isotopic fractionation factors, they found that CH_4 was near carbon isotopic equilibrium with CO_2 and hydrogen isotopic equilibrium with H_2O in some samples from marine sedimentary and CBG/SG fields. However, most samples from terrestrial environment and pure culture experiments do not achieve CH_4-CO_2/H_2O isotopic equilibrium. Turner et al. (2021) proposed that in low free energy gradient environments, high degrees of enzymatic reversibility in methanogenesis can catalyze carbon and hydrogen isotopic equilibrium of CO_2-CH_4-H_2O systems. However, it is difficult to identify under what conditions availability of free energy to microorganisms is low.

Currently, although carbon isotope equilibrium of CH_4-CO_2 has been observed in microbial CBG and SG basins, it is difficult to judge under what geological conditions equilibrium of CH_4 and CO_2 can be achieved. In addition, CO_2 is highly soluble in groundwater, the effects of dissolution on isotopic equilibrium and kinetic fractionation need to be considered (Chen et al., 2023). Many studies have shown that dissolved inorganic carbon (DIC) in the coproduced water of microbial CBG/SG is mainly from CO_2 dissolution (Golding et al., 2013). CH_4, CO_2 and DIC are the predominant carbon bearing components in CBG, SG and coexisting water systems. HCO_3^- is the dominant DIC species in most groundwater (Myrttinen et al., 2012). Therefore, we study the extent of carbon isotope fractionation in CH_4-CO_2-HCO_3^- systems in microbial CBG and SG basins. By comparing the differences between calculated isotopic equilibrium temperatures of samples and their present reservoir temperatures, we aim to quantify the importance of equilibrium and kinetic fractionation, and identify the reservoir conditions under which kinetic or equilibrium fractionation processes dominate. Important applications associated with equilibrium fractionation are also presented.

2. Samples

2.1 Sample sources

Samples collected and compiled in the study are from eight typical microbial CBG and SG basins (Fig. 1), where gas and coproduced water samples have been collected, and the geological and geochemical data of samples are more complete (See Supplementary Material). New samples were collected from the Erlian Basin, China (Fig. 1). Samples from existing literature that represent a range of gas formation depths and ages in the following reservoirs: the Fuxin Basin in China (Chen et al., 2023), the Powder River (Bates et al., 2011), the San Juan (Zhou et al., 2005), the Illinois (Schlegel et al., 2011), and the Michigan (Martini et al., 1998) Basins in USA, the Surat and the Clarence-Moreton Basins (Owen et al., 2016) in Australia.

2.2 Collection and analytical methods for samples from the Erlian Basin

Eight CBG and coproduced water samples from the Erlian Basin were collected directly from the CBG wellheads. Stainless steel cylinders with double valves were used to collect the CBG samples. After connecting a cylinder to the CBG pipeline at the wellhead, flushing the cylinder for 5mins to remove air and other contamination before sampling. Then filling up the cylinder with the CBG. Water samples were filtered via glass fiber filter membranes and were collected in 500mL glass bottles without headspace. Before sampling, these bottles were flushed three times repeatedly with coalbed water. In addition, four desorption gas samples from a coal core were collected at the drill site in the Erlian Basin. The sampling protocol is: quickly isolating the coal core into a gas desorption canister, closing and sealing the lid after filling the canister; after 3-4 minutes, opening the valve to discharge the gas mainly consisting of residual atmosphere,

reclosing the valve; after 48 hours, opening the valve to collect gas samples by displacement of saturated NaCl solution. The coal samples are collected to measure $\delta^{13}C_{coal}$ values.

Samples were analyzed at the Key Laboratory of Gas Geochemistry (Lanzhou), Institute of Geology and Geophysics, Chinese Academy of Sciences. The molecular components of the gas samples were analyzed by a MAT 271 trace gas mass spectrometer (Tao et al., 2007, 2020). Compared with the recognized atmosphere value, the spectrometer shows a very high precision, thus is suitable for the test of components of gas samples. The atmosphere sample measured on the apparatus had a slight difference of <0.3% for N_2 and O_2 contents, <0.02% for Ar, and 0.04 to 0.07% for CO_2, respectively.

The carbon and hydrogen isotope values of the gas, dissolved CH_4 and DIC samples were measured on a Gas Chromatograpy-Combustion-Isotope Ratio Mass Spectrometry (GC-C-IRMS). Trace GC 1310 gas chromatograph installed with HP-PlotQ type (50m×0.53mm×10μm) was used. The carrier gas was helium with a flow of 3mL/min and the inlet temperature was 200°C. The split ratio was 6:1. The GC oven conditions were initially held at 45ºC for 3mins, then heated to 240ºC at a rate of 15ºC/min and held for 20mins. For carbon isotope analysis, the oxidation furnace temperature was 945°C. For hydrogen isotope analysis, the cracking furnace temperature was 1450°C. The carbon isotope values were measured on Delta V Advantage IRMS and reported relative to Vienna Pee Dee Belemnite (VPDB), namely, $\delta^{13}C_S = (R_S/R_{VPDB}-1) \times 1000$, where R is the abundance ratio of ^{13}C and ^{12}C, S denotes the sample. The hydrogen isotope values were measured on MAT 253 IRMS and reported relative to Vienna Standard Mean Ocean Water (VSMOW), namely, $\delta D_S = (R_S/R_{VSMOW}-1) \times 1000$, where R is the abundance ratio of D and H, S denotes the sample. The precisions of $\delta^{13}C_S$ and δD_S are ±0.5‰ and ±2‰, respectively. The dissolved CH_4 samples were pretreated by heating its container to acquire

gaseous CH_4. DIC samples were pretreated by injecting pure phosphoric acid to acquire CO_2 (Li et al., 2007).

3. Calculation of equilibrium temperature in carbon isotopic exchange reactions of CH_4-CO_2-HCO_3^-

Typical carbon isotope exchange reactions among CH_4, CO_2 and HCO_3^- can be written as

$$^{12}CO_2 + {}^{13}CH_4 \leftrightarrow {}^{13}CO_2 + {}^{12}CH_4 \quad (1)$$

$$H^{12}CO_3^- + {}^{13}CO_2 \leftrightarrow H^{13}CO_3^- + {}^{12}CO_2 \quad (2)$$

$$H^{12}CO_3^- + {}^{13}CH_4 \leftrightarrow H^{13}CO_3^- + {}^{12}CH_4. \quad (3)$$

The equilibrium fractionation factors (or equilibrium constants) of the reactions (1-3) are temperature dependent (Urey, 1947; Myrttinen et al., 2012). In turn, the $\delta^{13}C$ values of CH_4, CO_2 and HCO_3^- can be used to calculate their equilibrium temperatures.

Experimental and theoretical studies (Bottinga, 1969; Richet et al., 1977; Horita, 2001; Kueter et al., 2019; Chen et al., 2019; Turner et al., 2021) have shown that the Urey model (Urey, 1947; Liu et al., 2010) of the reaction (1) is suitable for calculating thermodynamic isotope equilibration between CH_4 and CO_2. Based on Urey model, in order to accurately and conveniently calculate the equilibrium temperatures of the reaction (1), we updated Chen's code by comparing the temperatures calculated by Chen et al. (2019) and Turner et al. (2021) (See Supplementary Material).

Mook et al (1974) provided a reliable fit formular to calculate the equilibrium fractionation factors for the carbon isotopic exchange reaction between CO_2 and HCO_3^- in the temperature range of 0-125°C:

$$\varepsilon_{CO_2\text{-}HCO_3^-} = -\frac{9866}{T} + 24.12 \quad (4)$$

where $\varepsilon=1000(\alpha-1)$,

$$\alpha_{CO_2\text{-}HCO_3^-} = \frac{\delta^{13}C_{CO_2} + 1000}{\delta^{13}C_{HCO_3^-} + 1000} \quad (5)$$

We apply the formulars (4-5) to calculate the equilibrium temperature of the reaction (2).

Precise equilibrium temperatures for the exchange reaction (3) are difficult to achieve. We apply the relationships of equilibrium constants of reactions (1-3) to judge whether the calculated equilibrium temperature of the reaction (3) is consistent with the reservoir temperature of samples. We first used the $\delta^{13}C_{HCO3-}$ value and the reservoir temperature of sample to calculate the $\delta^{13}C_{CO2}$ value according the formulars (4-5), then we used the calculated $\delta^{13}C_{CO2}$ value and the $\delta^{13}C_{CH4}$ value of sample to calculate the equilibrium temperature. If the calculated temperature is consistent with the reservoir temperature, the HCO_3^- and CH_4 is close to carbon isotope equilibrium. According to the method, we develop a code in Matlab to calculate the equilibrium temperature (See Supplementary Material). By running the code and inputting a matrix consisted of reservoir temperatures, $\delta^{13}C_{HCO3-}$ values, and $\delta^{13}C_{CH4}$ values, the equilibrium temperature matrix can be calculated with an absolute error < 2°C.

4. Results

4.1 Geochemical composition and origin of CBG from the Erlian Basin

In Erlian Basin gas samples, CH_4 is the dominant gas phase with concentrations ranging from 94.6 to 96.8% (Table 1). The other significant component is CO_2, with concentrations of 3.2 to 3.9%. N_2 concentrations are from 0.0 to 1.5%. Ar concentrations are 0.02%. C_{2+} hydrocarbon gas concentrations are below detection limit (< 0.01%). Therefore, $C_{CH4}/(C_{C2H6} + C_{3C3H8})$ ratios are far greater than 1000, indicating the CBG in the Erlian Basin is dry gas, which is characteristic of microbial gas, late mature thermogenic gas, and/or abiotic gas (Milkov and Etiope, 2018). Erlian CBG samples are derived from coalbeds so they are unlikely to be abiotic in origin. The source coal is lignite with Ro values of 0.32-0.48%, indicating that these samples are not late mature thermogenic gas. Therefore, the CBG in the Erlian Basin is likely microbial in origin.

In the gas and water samples from production wells, $\delta^{13}C_{CH4}$ and $\delta^{13}C_{CH4(aq)}$ (dissolved CH_4) values are from -59.8 to -58.4‰ and -56.9 to -56.1‰, respectively, the average of $\delta^{13}C_{CH4(aq)}$-$\delta^{13}C_{CH4}$ is 2.6‰; $\delta^{13}C_{CO2}$ values are from -0.5 to 1.6‰ (Table 1). The small difference of $\delta^{13}C_{CH4}$ and $\delta^{13}C_{CH4(aq)}$ indicates that gaseous methane dissolution only has a small influence on its carbon isotopic composition. In desorption gas samples, $\delta^{13}C_{CH4}$ and δD_{CH4} values are from -60.6 to -56.2‰, and -267.2 to -239.2‰, respectively (Table 1). There is no significant difference in carbon and hydrogen isotopic compositions of methane samples between desorption gas and production gas. This characteristic suggests that $\delta^{13}C_{CH4}$ and δD_{CH4} values of the production gas and desorption gas from coal core are stable and can be used as an effective tracer of CBG (Tao et al., 2021).

Plots of $\delta^{13}C_{CH4}$ vs. δD_{CH4} and $\delta^{13}C_{CO2}$ vs. $\delta^{13}C_{CH4}$ are important tools for distinguishing origin of natural gases (Whiticar, 1999; Milkov and Etiope, 2018). In Fig. 2a, ($\delta^{13}C_{CH4}$ vs. δD_{CH4}), isotopic data of the gas samples fall in the common zone of microbial and thermogenic

gas. However, high $\alpha_{CO2\text{-}CH4}$ ($\alpha_{CO2\text{-}CH4} = (\delta^{13}C_{CO2} +1000)/(\delta^{13}C_{CH4} +1000)$) values of 1.059-1.065 (Table 1) suggest that the CBG samples are unlikely thermogenic, because the $\alpha_{CO2\text{-}CH4}$ value of thermogenic gas is generally less than 1.04 (Whiticar, 1999; Golding et al., 2013). Fig. 2b ($\delta^{13}C_{CO2}$ vs. $\delta^{13}C_{CH4}$) also shows that the CBG samples are mainly microbial in origin. High $\delta^{13}C_{DIC}$ values (15.1-15.7‰) of coproduced water provide further support for a microbial origin, because $\delta^{13}C$ of DIC from other origins are usually less than 2‰ (Golding et al., 2013). In the Erlian Basin, the coalbed water is Na-HCO_3-Cl type with pH values from 7.32-7.76 (Sun et al., 2018), which is favorable for biogenic methanogenesis. All evidence suggests that the Erlian CBG is mainly microbial gas.

The fractionation factor $\alpha_{CO2\text{-}CH4}$ is often employed to infer methanogenic pathways. The $\alpha_{CO2\text{-}CH4}$ values for CO_2 reduction and fermentations of acetate or methylated substrates are generally between 1.05 (or 1.06) and 1.09, and between 1.03 (or 1.04) and 1.06, respectively (Whiticar, 1999; Golding et al., 2013). In Erlian samples, $\alpha_{CO2\text{-}CH4}$ values are from 1.059 to 1.065, suggesting that the methanogenesis pathway is mainly CO_2 reduction (Fig. 3).

4.2 Origins and formation pathways of CBG and SG from other basins

Previous studies have reported that the CBG and SG in the Fuxin (Chen et al., 2023), the Powder River (Flores et al., 2008), the Illinois (Schlegel et al., 2011), the Michigan ((Martini et al., 1998), the Surat (Owen et al., 2016), and the Clarence-Moreton (Owen et al., 2016) Basins are mainly microbial gas, and CO_2 reduction is the dominant methanogenesis pathway. Fig. 2b shows that most of gas samples used in this study are mainly microbial gas. Moreover, high $\alpha_{CO2\text{-}CH4}$ values > 1.06 (except for the Fuxin and the San Juan samples) suggest that CO_2 reduction is the dominant methanogenesis pathway in these gases (Fig. 3).

For the Fuxin Basin samples, the $\alpha_{CO2\text{-}CH4}$ indicator is unreliable because stronger hydrodynamic activity in Fuxin coalbed aquifers has significantly affected the $\delta^{13}C_{CO2}$ values. Chen et al (2023) proposed that the groundwater flow has carried away ^{13}C-enriched CO_2 dissolved in coalbed water, leading to low $\delta^{13}C_{CO2}$ values and thus low $\alpha_{CO2\text{-}CH4}$ values in Fuxin CBG samples. In general, the $\Delta D_{H2O\text{-}CH4}$ ($\Delta D_{H2O\text{-}CH4}=\delta D_{H2O}-\delta D_{CH4}$) range associated with methanogenic pathway by CO_2 reduction is from 150 to 180‰ (Whiticar, 1999; Chen et al., 2023). In Fuxin samples, the $\Delta D_{H2O\text{-}CH4}$ values are from 148 to 178‰, suggesting that CO_2 reduction is the dominant methanogenic pathway in the Fuxin Basin.

Zhou et al. (2005) reported that the methane from the overpressured area of the San Juan Basin is dominantly microbial. High $\Delta^{13}C_{CO2\text{-}CH4}$ ($\Delta^{13}C_{CO2\text{-}CH4}=\delta^{13}C_{CO2}-\delta^{13}C_{CH4}$) values of 53.5 to 61.6‰ suggest that methanogenesis is mainly by CO_2 reduction. In the underpressured area of the basin, some samples fall into zone of the thermogenic gas in Fig. 2b. However, other samples fall into the zone of secondary microbial gas in Fig. 2b, indicating that the CBG in the area is likely a mixture of secondary microbial gas with thermogenic gas. Secondary microbial CBG can be generated after thermogenic CBG formation due to basin uplift and meteoric recharge. Microbial CBG from high-rank coalbeds with Ro greater than 0.5% is usually secondary microbial gas (Strąpoć et al., 2011). Primary microbial CBG is generated in the early stage of coalification with the Ro of the coal less than 0.4%. The coal Ro values in the San Juan Basin are greater than 0.5%, so the microbial CBG in the basin is secondary microbial gas.

4.3 Kinetic and equilibrium isotopic fractionations of CH_4-CO_2-HCO_3^- in microbial CBG and SG systems

Considering uncertainty from analytical measurement and theoretical calculation, we assume that CH_4-CO_2-HCO_3^- system in our samples is close to carbon isotope equilibrium when the absolute value of T-T_0 is less than or equal to 10°C, where T (including T_1, T_2, and T_3) and T_0 denote the isotope equilibrium temperature and the reservoir temperature, respectively (Figs. 4-6, Table 2). The T_1, T_2, and T_3 are calculated by the $\delta^{13}C$ values of CH_4-CO_2, $\delta^{13}C$ values of CH_4-DIC, and $\delta^{13}C$ values of CO_2-DIC, respectively. The reasons for the threshold of 10°C for T-T_0 are as followed. Considering the range of T_0 is about from 10°C to 45°C in our samples, we define that CH_4-CO_2-HCO_3^- system is near carbon isotopic equilibrium when the |T-T_0| value is less than 4°C if T and T_0 are exact values. However, there exists measured and calculated errors for T_0 and T. We assume that the error of measured T_0 is ±1°C, and the error of calculated T from theoretical equation is ±2°C. The uncertainty of measured $\delta^{13}C$ value of CH_4-CO_2-HCO_3^- system is ±0.5‰ (see Method section), the 1‰ error of $\delta^{13}C_{CO2}$-$\delta^{13}C_{CH4}$ under the range of 10-45°C can lead to < 3°C error. Therefore, the total error is about 10°C (4+1+2+3).

The calculated result shows that the extent of isotopic equilibrium of CH_4-CO_2 and CH_4-HCO_3^- is correlated with reservoir depth of CBG and SG in most samples (Figs. 4-5). For example, CH_4 is close to carbon isotopic equilibrium with CO_2 and/or HCO_3^- in most samples with relatively deep burial depths, such as, samples from the deep coalbeds of the Powder River, the San Juan, and the Surat/Clarence-Moreton Basins, as well from the deep shale rocks of the Illinois and the Michigan Basins (Figs. 4-5). These results not only support previous inferences that CH_4 and CO_2 can be near carbon isotopic equilibrium in microbial natural gas (Gropp et al., 2021; Turner et al., 2021), but also show CH_4 can be near carbon isotopic equilibrium with HCO_3^- in microbial natural gas. However, carbon isotopic equilibrium is not present between CH_4 and coproduced CO_2/HCO_3^- in most samples with shallow burial depths, such as, samples

from the shallow coalbeds of the Powder River, the Illinois, and the Surat/Clarence-Moreton Basins (Figs. 4-5). Most samples in this study are in CO_2-HCO_3^- carbon isotope disequilibrium (Fig. 6), so kinetic process largely controls carbon isotope fractionation between them.

5 Discussion

5.1 Geological controls on the isotopic fractionation of CH_4-CO_2 and CH_4-HCO_3^- in microbial CBG and SG basins

Both equilibrium and kinetic isotopic effects of CH_4-CO_2 have been observed in microbial CBG and SG basins (Turner et al., 2021). The availability of free energy to methanogens and anaerobic methanotrophs are often used to explain isotopic fractionation processes. When free energy gradients are low, enzymes catalyze reactions are reversible, thus can catalyze both the forward reduction of CO_2 to CH_4 and the reverse oxidation of CH_4 back to CO_2. This reversibility promotes carbon isotope exchange reactions between CH_4 and CO_2, and leads to isotopic equilibration (Valentine et al., 2004; Stolper et al., 2014; Yoshinaga et al., 2014; Turner et al., 2021). In contrast, high free energy gradients lead to enzymes catalyze reactions are wholly or partially irreversible, and only can catalyze the forward reduction of CO_2 to CH_4, thus lead to kinetic isotopic fractionation of CH_4-CO_2. In general, in microbial CBG/SG system, available organic carbon is less reactive, which could result in low free energy gradients for methanogens and thus promote isotope exchange reaction of CH_4-CO_2.

In the most methane samples used in this study, methanogenesis pathway is mainly CO_2 reduction, and anaerobic methanotrophs is insignificant. According to previous interpretation, during CO_2 reduction to CH_4 in the CBG and SG reservoirs, CO_2 (including gaseous and

293 dissolved CO_2) content is high, but H_2 content is very limited (Vinson et al., 2017; Turner et al.,
294 2021). Low H_2 content is favorable for isotopic equilibrium of CH_4-CO_2, because, at low free
295 energy gradients (i.e., low H_2 content), the enzymes of methanogens are fully reversible,
296 promoting isotopic equilibrium of CH_4-CO_2 (Valentine et al., 2004; Wang et al., 2015; Okumura
297 et al., 2016; Gropp et al., 2021). Rhim and Ono (2022) proposed that low dissolved H_2 promote
298 isotopic equilibrium of CH_4-CO_2. However, in most samples with shallow burial depths, carbon
299 isotopic equilibrium is not present between CH_4 and CO_2 (Fig. 4). Laboratory methanogen
300 cultures also show that CH_4 and CO_2 are out of isotopic equilibrium even at low H_2 content
301 (Okumura et al., 2016; Turner et al., 2021; Rhim and Ono, 2022). We propose that besides low
302 free energy gradient (i.e., low gaseous and/or dissolved H_2 content), longterm coexistence of
303 CH_4-CO_2 is necessary to attain isotopic equilibrium in microbial CBG and SG systems due to
304 isotope exchange rate between CH_4 and CO_2 in these systems are very sluggish (Games and
305 Hayes, 1976; Whiticar et al., 1986).
306 Coalbeds and organic-rich shales serving as both source rocks and reservoirs of CBG and SG
307 are tight with low permeability. They can provide sealed reservoirs for CBG and SG storage. If
308 the reservoirs of microbial CBG and SG are geologically and geochemically stable over a long
309 timescale, isotope exchange reaction of CH_4 and CO_2/HCO_3^- catalyzed by methanogenic
310 microbial metabolism is likely to attain equilibrium (Okumura et al., 2016, Turner et al., 2021).
311 However, if the reservoirs are relatively open and unstable, many processes or factors such as,
312 short coexistence time of CH_4-CO_2-HCO_3^-, mixing between microbial and thermogenic gas,
313 strong hydrodynamic activity, and anaerobic methane oxidation can significantly affect the
314 concentrations and isotopic compositions of CH_4-CO_2-HCO_3^- (Vinson et al., 2017). In this case,
315 the system is unlikely to attain equilibrium.

316 In the Erlian Basin, CBG was from the Lower Cretaceous Saihantala Formation (K_{1s}).
317 During and after the K_{1s} deposition, the basin has been more stable. In the sampling area, the
318 CBG with burial depths of 450-600m were well sealed by thick coalbeds, regionally confined
319 water, and thick mudstone caprocks (Sun et al., 2018). The conditions are favorable for
320 conservation of the CBG, providing sufficient time for the isotopic equilibrium between CH_4 and
321 CO_2/HCO_3^-. However, in relatively high-pressure and closed CBG reservoirs in the basin, high
322 CO_2 solubility can lead to most of CO_2 dissolved into groundwater to form DIC, and thus lead to
323 low abundance CO_2 in CBG and high abundance CO_2 (DIC) in coalbed water. However,
324 groundwaters insignificantly affect the abundance and carbon isotope composition of CH_4 due to
325 low CH_4 solubility (Chen et al., 2023). Some CO_2 exsolution resulting from the reduction of
326 reservoir pressure in CBG recovery may significantly affect the $\delta^{13}C$ of CO_2, but insignificantly
327 affect $\delta^{13}C$ of DIC and CH_4, thus, CH_4-HCO_3^- is close to isotope equilibrium, but CO_2-HCO_3^-
328 and CH_4-CO_2 are in isotope disequilibrium (Figs. 4-6). For CBG and water samples from the
329 Fuxin Basin, CH_4-CO_2-HCO_3^- system is in isotope disequilibrium at present reservoir conditions
330 (Figs. 4-6) because the groundwater flow in Fuxin coalbeds has carried away ^{13}C-enriched CO_2
331 dissolved in coalbed water, thus cause low $\delta^{13}C_{CO2}$ and $\delta^{13}C_{DIC}$, leading to disequilibrium of
332 CH_4-CO_2-HCO_3^- system (Chen et al., 2023).
333 In the San Juan Basin, high production CBG wells are located in the overpressured region of
334 the basin, while low production CBG wells are in the underpressured region. Overpressure is the
335 result of recharge at an elevated outcrop on the basin margin, aquifer confinement by the
336 Kirtland Shale and low-permeability Pictured Cliffs Sandstone, and basinward pinch-out of
337 aquifer coalbeds (Scott et al., 1994). The hydrodynamic seal is favourable for the CBG
338 accumulation and long storage in the deep and overpressured coalbeds, thus, the CH_4 and CO_2

339 /HCO_3^- is near isotopic equilibrium (Figs. 4-5). However, the relatively shallow and
340 underpressured coalbeds are unfavourable for long conservation of CBG. The processes, such as
341 CBG migration out of coalbeds and mixture of thermogenic and microbial gas, may cause CH_4
342 and CO_2 disequilibrium in some samples (Fig. 4).
343 For the Surat/Clarence-Moreton Basin samples, the deep CBG reservoirs (200-500m) are in a
344 closed-system and trapped on stable geological structures (Owen et al., 2016), favourable for the
345 CBG storage and accumulation. Hence, the coexistence of the CH_4 and HCO_3^- is long enough to
346 allow equilibrium to be reached (Fig. 5). However, the shallow CBG reservoirs (< 200m), which
347 are directly underlying or adjacent to the alluvium, are not ideal for the accumulation of CBG.
348 Sulfate reduction and various methanogenic pathways may have largely affected the contents and
349 isotopic compositions of CH_4 and HCO_3^- (Owen et al., 2016). Under these geological conditions,
350 CH_4 and HCO_3^- is unlikely to attain equilibrium (Fig. 5). In contrast, deep, closed reservoir
351 conditions in the Powder River, the Illinois and the Michigan Basins are conducive to obtaining
352 isotopic equilibrium between CH_4 and CO_2/HCO_3^- (Figs. 4-5). For the Powder River samples,
353 the extent of isotopic equilibrium of CH_4-CO_2 and CH_4-HCO_3^- in deep and closed coalbeds (203-
354 475m) is higher than that in shallow coalbeds (98-310m). In the Illinois Basin, the extent of
355 isotopic equilibrium of CH_4-CO_2 and CH_4-HCO_3^- in shale reservoirs with depths of 233-857m is
356 higher than that in coalbeds with depths of 135-402m. In the Michigan Basin, the relatively deep
357 (200-650m) and geologically stable shale reservoirs are favourable for the SG accumulation and
358 long storage, thus the extent of isotopic equilibrium of CH_4-CO_2 and CH_4-HCO_3^- is high.
359 Overall, we proposed that a relatively deep and closed CBG/SG reservoir is geologically and
360 geochemically stable over long timescales, and thus is favourable for isotopic equilibrium of
361 CH_4-CO_2/HCO_3^-. However, it is difficult to accurately estimate the timescale for attaining carbon

362 isotopic equilibrium of CH_4-CO_2 and CH_4-HCO_3^- in our samples. In complex microbial CBG
363 and SG environments, the rates of carbon isotope exchange of CH_4-CO_2 and CH_4-HCO_3^- are
364 unlikely to be estimated. This is because the rates depend on the structure of the enzyme
365 catalyzing reactions, and on the exact substrates participating in the reactions (Gropp et al.,
366 2021). We have also not known that isotopic equilibrium of CO_2-CH_4 and CH_4-HCO_3^- occurred
367 in methane formation process or after methane formation (Turner et al., 2021).
368 However, it is possible to roughly estimate the timescale for attaining isotope equilibrium of
369 CH_4-CO_2 and CH_4-HCO_3^- in our samples. For microbial CBG and SG samples used in the study,
370 their formation time is significantly later than the time of their reservoir formation. This is
371 because most of them formed after re-inoculation of coalbeds and shale rocks with methanogenic
372 microbial consortia via meteoric water recharge (Bates et al., 2011; Chen et al., 2023; Martini et
373 al., 1998; Owen et al., 2016; Schlegel et al., 2011; Scott et al., 1994). For example, methanogenic
374 microbes in Pennsylvanian coalbeds and upper Devonian shale rocks (Table 2) in the Illinois
375 Basin mainly originated from recent meteoric water recharge (<2 Ma) (Schlegel et al., 2011).
376 Therefore, the isotope equilibrium time of CO_2-CH_4 and CH_4-HCO_3^- is less than 2 Ma in the
377 basin. Similarly, the equilibrium time of CO_2-CH_4 and CH_4-HCO_3^- is less than 21,000 years in
378 the Michigan Basin (Martini et al., 1998), less than 50,000 years in the Powder River (Bates et
379 al., 2011) and the Surat Basin (Baublys et al., 2015).
380
381 5.2 Kinetic carbon isotope fractionation of CO_2-HCO_3^- in microbial CBG and SG systems
382 When the $\delta^{13}C$ value of gaseous CO_2 is unknown in microbial gas basins, many studies often
383 used the $\delta^{13}C$ value of the coexisting DIC to estimate the $\delta^{13}C_{CO2}$ under the assumptions that

384 HCO_3^- is the predominant DIC species, and HCO_3^- is in carbon isotope equilibrium with CO_2
385 (Bates et al., 2011; Turner et al., 2021). However, this assumption needs to be verified.
386 In general, HCO_3^- is the dominant DIC species in groundwaters. Because the pH values of
387 most groundwaters are often between 6.4 and 10.3, where HCO_3^- is the dominant DIC species
388 (Myrttinen et al., 2012). However, from our calculated results, CO_2 and HCO_3^- are not in carbon
389 isotope equilibrium in most of samples (Fig. 6). Therefore, it is unreasonable to assume that
390 CO_2-HCO_3^- is near isotopic equilibrium in microbial CBG/SG systems. As a result, the estimated
391 $\delta^{13}C_{CO2}$ value based on isotopic equilibrium of CO_2-HCO_3^- may be unreliable.
392 Experimental studies have shown that the rates of carbon isotope exchange between
393 individual DIC species (H_2CO_3, HCO_3^-, CO_3^{2-}) and gaseous CO_2 are rapid even at low
394 temperature range of 0-100°C, because their isotopic equilibrium can be reached in time periods
395 of several hours to several days (<30 days) (Myrttinen et al., 2012). The rapid exchange rates
396 suggest that although the carbon isotope equilibrium of CO_2-HCO_3^- is easy to achieve in
397 microbial CBG and SG reservoirs, the equilibrium is unstable.
398 CBG and SG recovery by dewatering and/or fracturing to reduce the reservoir pressure can
399 cause CO_2 exsolution which may break isotope equilibrium of CO_2-HCO_3^-. High CO_2 solubility
400 can lead to most of CO_2 dissolved into groundwater to form DIC, thus, lead to low abundance
401 CO_2 in CBG and SG (typical < 5%) and high abundance CO_2 (i.e., DIC) in groundwaters (Chen
402 et al., 2023). Hence, some CO_2 exsolution may significantly affect the $\delta^{13}C$ of CO_2, but
403 insignificantly affect $\delta^{13}C$ of DIC, causing isotope disequilibrium of CO_2-HCO_3^-. The
404 mechanism may explain the carbon isotope disequilibrium of CO_2-HCO_3^- in our samples.
405
406 5.3 Estimation of total yield ratio of CO_2/CH_4 in microbial CBG reservoirs

Large amounts of CH_4 and CO_2 can be formed during microbial conversion of coal into natural gas. Knowing the total yield ratio of CO_2/CH_4 is critical for elucidating the formation mechanisms and predicting emissions to atmosphere. However, it is often difficult to estimate their yield ratio *in situ* coalbeds, because several processes can significantly affect their yields. These include mixing between microbial and thermogenic gas, extent of methanogenesis, migrations, methane oxidation, CO_2 dissolution, and precipitation and dissolution of carbonate minerals (Vinson et al., 2017). Based on carbon isotope equilibrium of CH_4-CO_2 and CH_4-HCO_3^-, we estimate CO_2 percentage in total CH_4 and CO_2 in microbial CBG reservoir, where methanogenesis pathway is mainly CO_2 reduction.

In the subsurface, dissolution of CO_2 can significantly affect the abundance and isotopic compositions of gaseous CO_2 due to its high solubility (Chen et al., 2023). Gilfillan et al. (2009) suggested that solubility trapping in formation water was the dominant CO_2 sink. The $\delta^{13}C_{DIC}$ values of most samples used in this study are greater than 5‰, which suggest strongly that the DIC is mainly from CO_2 dissolution, because $\delta^{13}C$ of DIC from other origins are usually less than 2‰ (Golding et al., 2013). Furthermore, the solubility of CO_2 could be more than 10 times that of CH_4 under certain temperature, pressure and salinity conditions (Fig. 7a). In the coalbed water from the Surat/Clarence-Moreton Basin, the concentration of HCO_3^- is dozens of times that of dissolved CH_4 (Fig. 7b). Large amounts of water are often produced in CBG recovery (Hamawand et al., 2013; Meng et al., 2014), suggesting that significant CO_2 dissolution occurs in groundwater associated with coalbeds. Hence, we propose that the dominant states of CO_2 in CBG reservoirs are gaseous and dissolved states. However, the dominant state of CH_4 is gaseous due to its low solubility.

Many studies have shown that $\delta^{13}C_{coal}$ is stable, coal rank has negligible effect to $\delta^{13}C_{coal}$ (Whiticar, 1996; Rahman et al., 2017). For example, the range of Ro of 5# coalbed from the Illinois Basin is from 0.55% to 4.79%. However, the range of $\delta^{13}C_{coal}$ is only from -25.3‰ to -24.9‰ (Rahman et al., 2017). The Ro values of Huangxian coal increase from 0.39% to 1.79% in pyrolysis experiments but, the $\delta^{13}C_{coal}$ variability is only 0.26‰ (Lu et al., 1994). We assumed that $\delta^{13}C$ values of coals were invariable during microbial CBG formation. Because the dominant products are CH_4 and CO_2 during microbial CBG formation, and the $\delta^{13}C_{coal}$ value is usually greater than the $\delta^{13}C_{CH4}$ value, but smaller than the $\delta^{13}C_{CO2}$ value, therefore, we propose that the formation of ^{13}C-depleted CH_4 and ^{13}C-enriched CO_2 make $\delta^{13}C$coal stable.

Based on the above analysis and discussion that 1) dominant state of CH_4 in coalbed reservoirs is gaseous, and dominant states of CO_2 are gaseous and dissolved; 2) The formations of ^{13}C-depleted CH_4 and ^{13}C-enriched gaseous and dissolved CO_2 make $\delta^{13}C_{coal}$ stable; 3) Existing of isotopic equilibrium of CH_4-CO_2 and/or CH_4-HCO_3^- suggests that the CBG reservoir has been more closed, thus, the primary microbial CH_4 and CO_2 are likely to be well retained *in situ* coalbeds. Therefore, we can apply the gas and water samples in which CH_4-CO_2 and/or CH_4-HCO_3^- are near isotope equilibrium to estimate the CO_2 percentage in total CH_4 and CO_2 in microbial CBG basin by the following formulas

$$f\,\delta^{13}C_{CO2} + (1-f)\,\delta^{13}C_{CH_4} \approx \delta^{13}C_{coal} \quad (6)$$

$$f\,\delta^{13}C_{DIC} + (1-f)\,\delta^{13}C_{CH_4} \approx \delta^{13}C_{coal} \quad (7)$$

where f is CO_2 percentage ($X_{CO2}/(X_{CO2}+X_{CH4})$) in total CH_4 and CO_2. In microbial CBG reservoirs, the $\delta^{13}C_{DIC}$ is usually greater than that of CO_2, therefore, the calculated f using the equations (6) and (7) represent the upper and lower limits of $X_{CO2}/(X_{CO2}+X_{CH4})$, respectively.

In each basin, the average isotopic values ($^{13}C_{CH4}$, $\delta^{13}C_{CO2}$, $\delta^{13}C_{DIC}$ and $\delta^{13}C_{coal}$) of samples near isotope equilibrium of CH_4-CO_2 and/or CH_4-HCO_3^- are used to estimate $X_{CO2}/(X_{CO2}+X_{CH4})$ values. In these basins, the estimated lower limits of $X_{CO2}/(X_{CO2}+X_{CH4})$ are from 27% to 50%, which are significantly higher than the $CO_2/(CH_4+CO_2)$ values of 1-15% in CBG samples (Table 3). However, the $X_{CO2}/(X_{CO2}+X_{CH4})$ values are consistent with the $CO_2/(CH_4+CO_2)$ values from culture experiments for conversion of coal to methane. For example, culture experiments using bituminous coal as the sole carbon source and the microorganisms from the CBG coproduced waters from the Illinois Basin, USA produced CH_4 and CO_2, whose yields are 3.14m^3/ton/day and 2.58m^3/ton/day in 20 days, respectively (Zhang et al., 2015). The ratio of $CO_2/(CO_2+CH_4)$ is 38%. Water and coal samples from a CBG well in the Jharia block, India yielded $CO_2/(CH_4+CO_2)$ ratio of 39% (Rathi et al., 2019). And culture experiments using anthracite coal and water samples from the Qinshui Basin, China produced average yield $CO_2/(CH_4+CO_2)$ ratios of 36% to 48% (Xiao et al, 2013). In relatively high-pressure and closed CBG reservoirs, high CO_2 solubility and low CH_4 solubility can cause low CO_2 content, high CH_4 content, and thus low $CO_2/(CH_4+CO_2)$ ratio in CBG. However, the extent of the dissolution of both CO_2 and CH_4 are low in culture experiments due to low-pressure conditions and short experiment timescales. For this reason, the $CO_2/(CH_4+CO_2)$ values from culture experiments are consistent with the $X_{CO2}/(X_{CO2}+X_{CH4})$ values from the field samples. This consistence also suggests that our estimated values are more reliable.

The percentage of dissolved CO_2 in total CO_2 (including gaseous and dissolved CO_2) is estimated by using the formula

$$f_1 = 1 - \frac{1/m - 1}{1/n - 1} \quad (8)$$

where m and n denote the $X_{CO2}/(X_{CO2}+X_{CH4})$ values and the $CO_2/(CH_4+CO_2)$ values, respectively. The results show that 53-99% of the CO_2 has dissolved into groundwaters to form DIC in CBG reservoirs (Table 3). Therefore, we propose that CO_2 dissolution likely has significantly affect the abundance and isotopic compositions of gaseous CO_2 in subsurface.

6 Conclusions and outlook

This study supports previous inferences that CH_4 and CO_2 can be near carbon isotopic equilibrium in microbial CBG and SG basins. It also suggests that CH_4 and HCO_3^- can be near carbon isotopic equilibrium in these basins. However, CO_2 and HCO_3^- are not in carbon isotopic equilibrium in these basins. We propose that, low free energy gradients (i.e., low H_2 content) and long coexistence time of CH_4-CO_2-HCO_3^- are necessary to achieve isotopic equilibrium. In general, a relatively deep and closed CBG/SG reservoir is geologically and geochemically stable over long timescales, favoring isotopic equilibrium of CH_4-CO_2 and CH_4-HCO_3^-. However, it is difficult to accurately estimate the timescale for attaining equilibrium of CH_4 and CO_2/HCO_3^- in natural samples. Conversely a shallow and open CBG/SG reservoir where CH_4 and CO_2/HCO_3^- coexist for shorter time periods is unfavourable for their isotopic equilibrium. We estimated the lower limits of the percentage of CO_2 in total CH_4 and CO_2 in CBG reservoirs in various basins to be from 27% to 50%, where methanogenesis is mainly by CO_2 reduction. However, the 53-99% CO_2 have dissolved into groundwaters to form DIC in CBG reservoirs. CO_2 dissolution could significantly affect abundance and isotopic compositions of CO_2 in CBG. CO_2 dissolution effect in natural gas geochemistry needs to be studied further.

This study and previous studies (Valentine et al., 2004; Gropp et al., 2021; Turner et al., 2021) show that CH_4 formed mainly by CO_2 reduction can be near carbon and hydrogen isotopic equilibrium with coexisting CO_2, HCO_3^- and H_2O in natural gas reservoirs. However, it is not clear whether CH_4 formed by acetoclastic or methylotrophic can be near isotopic equilibrium with coexisting CO_2, HCO_3^- and H_2O in subsurface. If methanogenesis pathways have a weak influence on isotopic equilibrium of CH_4-CO_2-HCO_3^--H_2O system, the empirical isotopic proxies, such as, $\alpha_{CO2\text{-}CH4}$ and $\Delta D_{H2O\text{-}CH4}$, for distinguishing methanogenesis pathways would not be reliable because under the equilibrium condition, $\alpha_{CO2\text{-}CH4}$ and $\Delta D_{H2O\text{-}CH4}$ are mainly dependent on temperature rather than methanogenesis pathways.

Author Contributions

X.C., M.T. and Z.Z. designed this research project. X.C. and M.T collected and analyzed samples. X.C. and Z.Z wrote the paper. Y.W. and G.H. made significant contribution in data interpretation and discussion.

Declaration of competing interest

The authors declare that they have no known competing financial interests or personal relationships that could have appeared to influence the work reported in this paper.

Acknowledgments

We thank Yuzhen Ma, Zhongping Li and Qian Wang for assistance in sample collection and measurement. We thank Hongyan Ma and Zhao Huang for assistance in drawing map. Thanks to

Huabei Oilfield Company. This research was funded by the National Natural Science Foundation of China (41772122), China Postdoctoral Science Foundation (2021M703223), Project of Stable Support for Youth Team in Basic Research Field, CAS (YSBR-017), the Strategic Priority Research Program of the Chinese Academy of Sciences (XDA14010103), National Key Research and Development Plan of China (2017YFC1503004-03), and Natural Environment Research Council of UK (Grant Ref: NE/T004452/1).

Supplementary Material

Supplementary Material included Research Data is available in the attachment.

References

Akinfiev, N.N., Diamond, L.W., 2010. Thermodynamic model of aqueous CO_2–H_2O–NaCl solutions from -22 to 100°C and from 0.1 to 100 MPa. Fluid Phase Equilibr. 295, 104-124.

Bates, B.L., McIntosh, J.C., Lohse, K.A., Brooks, P.D., 2011. Influence of groundwater flowpaths, residence times and nutrients on the extent of microbial methanogenesis in coal beds: Powder River Basin, USA. Chem. Geol. 284, 45–61.

Baublys, K.A., Hamilton, S.K., Golding, S.D., Vink, S., Esterle, J., 2015. Microbial controls on the origin and evolution of coal seam gases and production waters of the Walloon Subgroup; Surat Basin, Australia. Int. J. Coal Geol. 147, 85–104.

Bottinga, Y., 1969. Calculated fractionation factors for carbon and hydrogen isotope exchange in the system calcite-carbon dioxide-graphite-methane-hydrogen-water vapor. Geochim. Cosmochim. Acta 33, 49–64.

Chen, X., Tao, M., Zhou, Z., Li, D., 2019. A new theoretical calculation of the equilibrium constant and temperature for the carbon isotope exchange reaction between CH_4 and CO_2. Geothermics 79, 140–144.

Chen, X., Wang, Y., Tao, M., Zhou, Z., He, Z., Song, K., 2023. Tracing the origin and formation mechanisms of coalbed gas from the Fuxin Basin in China using geochemical and isotopic signatures of the gas and coproduced water. Int. J. Coal Geol. 267, 104185.

Diamond, L.W., Akinfiev, N.N., 2003. Solubility of CO_2 in water from -1.5 to 100°C and from 0.1 to 100 MPa: evaluation of literature data and thermodynamic modelling. Fluid Phase Equilibr. 208, 265-290.

Duan, Z., Møller, N., Greenberg, J., Weare, J. H., 1992. The prediction of methane solubility in natural waters to high ionic strength from 0 to 250°C and from 0 to 1600 bar. Geochim. Cosmochim. Acta 56, 1451-1460.

Flores, R.M., Rice, C.A., Stricker, G.D., Warden, A., Ellis, M.S., 2008. Methanogenic pathways of coal-bed gas in the Powder River Basin, United States: The geologic factor. Int. J. Coal Geol. 76, 52–75.

Games L. M., Hayes J. M., 1976. Isotopic and quantitative analysis of the major carbon fractions in natural water samples. Anal. Chem. 48, 130–135.

Gilfillan, S.M., Lollar, B.S., Holland, G., Blagburn, D., Stevens, S., Schoell, M., Cassidy, M., Ding, Z., Zhou, Z., Lacrampe-Couloume, G., Ballentine, C., 2009. Solubility trapping in formation water as dominant CO_2 sink in natural gas fields. Nature 458, 614–618.

Golding, S.D., Boreham, C.J., Esterle, J.S., 2013. Stable isotope geochemistry of coal bed and shale gas and related production waters: A review. Int. J. Coal Geol. 120, 24–40.

Gropp, J., Iron, M.A., Halevy, I., 2021. Theoretical estimates of equilibrium carbon and

564 hydrogen isotope effects in microbial methane production and anaerobic oxidation of
565 methane. Geochim. Cosmochim. Acta 295, 237–264.
566 Hamawand, I., Yusaf, T., Hamawand, S.G., 2013. Coal seam gas and associated water: a review
567 paper. Renew. Sust. Energ. Rev. 22, 550–560.
568 Horita, J., 2001. Carbon isotope exchange in the system CO_2-CH_4 at elevated temperatures.
569 Geochim. Cosmochim. Acta 65, 1907–1919.
570 Kueter, N., Schmidt, M.W., Lilley, M.D., Bernasconi, S.M., 2019. Experimental determination
571 of equilibrium CH_4–CO_2–CO carbon isotope fractionation factors (300–1200°C). Earth
572 Planet. Sci. Lett. 506, 64–75.
573 Li, Z. Tao, M., Li, L., Wang, Z., Du, L., Zhang, M., 2007. Determination of isotope composition
574 of dissolved inorganic carbon by gas chromatography-conventional isotope-ratio mass
575 spectrometry. Chin. J. Anal Chem. 35, 1455–1458.
576 Liu, Q., Tossell, J. A., Liu, Y., 2010. On the proper use of the Bigeleisen-Mayer equation and
577 corrections to it in the calculation of isotopic fractionation equilibrium constants. Geochim.
578 Cosmochim. Acta 74, 6965–6983.
579 Lu, S., Huang, D., Cheng, K., 1994. Characteristics of solid residue samples and its evolution in
580 a simulation experiment of generation and migration of coal formed hydrocarbon (in
581 Chinese). Petrol Explor Dev. 21, 46–51.
582 Martini, A.M. Walter, L.M., Budai, J.M., Ku, T.C.W., Kaiser, C.J., Schoell. M., 1998. Genetic
583 and temporal relations between formation waters and biogenic methane: Upper Devonian
584 Antrim Shale, Michigan Basin, USA. Geochim. Cosmochim. Acta 62, 1699–1720.
585 Meister, P., Liu, B., Khalili, A., Bottcher, M.E., Jørgensen, B.B., 2019. Factors controlling the
586 carbon isotope composition of dissolved inorganic carbon and methane in marine

porewater: An evaluation by reaction-transport modelling. J. Mar. Syst. 200, 103227.

Meng, Y., Tang, D., Xu, H., Li, Y., Gao, L., 2014. Coalbed methane produced water in China: status and environmental issues. Environ. Sci. Pollut. Res. 21, 6964–6974.

Milkov, A.V., Etiope, G., 2018. Revised genetic diagrams for natural gases based on a global dataset of >20,000 samples. Org. Geochem. 125, 109–120.

Mook, W.G., Bommerson, J.C., Staverman, W.H., 1974. Carbon isotope fractionation between dissolved bicarbonate and gaseous carbon dioxide. Earth Planet. Sci. Lett. 22, 169–176.

Myrttinen, A., Becker, V., Barth, J.A.C., 2012. A review of methods used for equilibrium isotope fractionation investigations between dissolved inorganic carbon and CO_2. Earth-Sci Rev.115, 192–199.

Okumura, T., Kawagucci, S., Saito, Y., Matsui, Y., Takai, K., Imachi, H., 2016. Hydrogen and carbon isotope systematics in hydrogenotrophic methanogenesis under H_2-limited and H2-enriched conditions: implications for the origin of methane and its isotopic diagnosis. Prog. Earth Planet. Sci. 3, 1–19.

Owen, D.D.R., Shouakar-Stash, O., Morgenstern, U., Aravena, R., 2016. Thermodynamic and hydrochemical controls on CH_4 in a coal seam gas and overlying alluvial aquifer: New insights into CH_4 origins. Sci. Rep 6, 1–20.

Rahman, M.W., Rimmer, S.M., Rowe, H. D., Huggett, W.W., 2017. Carbon isotope analysis of whole-coal and vitrinite from intruded coals from the Illinois Basin: No isotopic evidence for thermogenic methane generation. Chem Geol, 453, 1-11.

Rathi, R., Lavania, M., Singh, N., Sarma, P. M., Kishore, P., Hajra, P., Lal, B., 2019. Evaluating indigenous diversity and its potential for microbial methane generation from thermogenic coal bed methane reservoir. Fuel, 250, 362–372.

610 Rhim, J.H., Ono, S., 2022. Combined carbon, hydrogen, and clumped isotope fractionations
611 reveal differential reversibility of hydrogenotrophic methanogenesis in laboratory cultures.
612 Geochim. Cosmochim. Acta 335, 383–399.
613 Richet, P, Bottinga, Y., Javoy, M. A., 1977. Review of Hydrogen, Carbon, Nitrogen, Oxygen,
614 Sulphur, and Chlorine Stable Isotope Fractionation Among Gaseous Molecules. Annu. Rev.
615 Earth Planet. Sci. 5, 65–110.
616 Schlegel, M.E., Mcintosh, J.C., Bates, B.L., Kirk, M.F., Martini, A.M., 2011. Comparison of
617 fluid geochemistry and microbiology of multiple organic-rich reservoirs in the Illinois Basin
618 , USA : Evidence for controls on methanogenesis and microbial transport. Geochim.
619 Cosmochim. Acta 75, 1903–1919.
620 Scott, A.R., Kaiser, W.R., Ayers Jr, W.B., 1994. Thermogenic and secondary biogenic gases,
621 San Juan basin, Colorado and New Mexico-implications for coalbed gas producibility.
622 AAPG bull. 78, 1186–1209.
623 Smith J. W., Gould K. W., Rigby D., 1981. The stable isotope geochemistry of Australian coals.
624 Org. Geochem. 3, 111–131.
625 Stolper D., Lawson M., Davis C. L., Ferreira A. A., Santos Neto E. V., Ellis G. S., Lewan M. D.,
626 Martini A. M., Tang,Y., Schoell M., Sessions A. L., Eiler J. M., 2014. Formation
627 temperatures of thermogenic and biogenic methane. Science 344, 1500–1503.
628 Sun, H., 2015. The simulation of coal reservoir soluble gas and research on hydrogeologic gas
629 controlling in Fukang Mining Area (in Chinese) [D]. China University of Mining and
630 Technology. 57-58.
631 Sun, Q., Wang, W., Tian, W., Sun, B., Chen, Y., Yang, Q., Chen, H., Yang, M., Qi, L., 2018.
632 Accumulation patterns of low-rank coalbed methane gas in the Jiergalangtu Sag of the

633 Erlian Basin (in Chinese). Nat. Gas Ind. 38, 59–66.
634 Suto, N., Kawashima, H., 2016. Global mapping of carbon isotope ratios in coal. J Geochem
635 Explor, 167, 12–19.
636 Tao, M., Chen, X., Li, Z., Ma, Y., Xie, G., Wang, Y., Wei, L., Wang, A., Huang, Z., 2021.
637 Variation characteristic and mechanism of carbon isotope composition of coalbed methane
638 under different conditions and its tracing significance. Fuel, 302, 1–9.
639 Tao, M., Chen, X., Ma, Y., Wang, Y., Li, Z., Xiao, W., Huang, Z., 2020. Geological–
640 Geochemical models and isotope fractionation laws and control factors of thermogenic
641 coalbed gas in Panxian, China. Energy Fuels, 34, 2665-2673.
642 Tao, M., Shi, B., Li, J., Wang, W., Li, X., Gao, B., 2007. Secondary biological coalbed gas in the
643 Xinji area, Anhui province, China: Evidence from the geochemical features and secondary
644 changes. Int. J. Coal Geol. 71, 358–370.
645 Turner, A.C., Korol, R., Eldridge, D.L., Bill, M., Conrad, M., Miller, T.F., Stolper, D.A., 2021.
646 Experimental and theoretical determinations of hydrogen isotopic equilibrium in the system
647 CH_4-H_2-H_2O from 3 to 200°C. Geochim. Cosmochim. Acta 314, 223–269.
648 Urey, H.C., 1947. The thermodynamic properties of isotopic substances. J. Chem. Soc (Lond.).
649 562–581.
650 Valentine, D.L., Chidthaisong, A., Rice, A., Reeburgh, W.S., Tyler, S.C., 2004. Carbon and
651 hydrogen isotope fractionation by moderately thermophilic methanogens. Geochim.
652 Cosmochim. Acta 68, 1571–1590.
653 Vinson, D.S., Blair, N.E., Martini, A.M., Larter, S., Orem, W.H., McIntosh, J.C., 2017.
654 Microbial methane from in situ biodegradation of coal and shale: A review and reevaluation
655 of hydrogen and carbon isotope signatures. Chem. Geol. 453,128–145.

Wang, D.T., Gruen, D.S., Sherwood Lollar, B., Hinrichs, K.U., Stewart, L.C., Holden, J.F., Hristov, A.N., Pohlman, J.W., Morrill, P.L., Könneke, M., Delwiche, K.B., Reeves, E.P., Sutcliffe, C.N., Ritter, D.J., Seewald, J.S., McIntosh, J.C., Hemond, H.F., Kubo, M.D., Cardace, D., Hoehler, T.M., Ono, S., 2015. Nonequilibrium clumped isotope signals in microbial methane. Science 348, 428–431.

Whiticar, M.J., 1999. Carbon and hydrogen isotope systematics of bacterial formation and oxidation of methane. Chem. Geol. 161, 291-314.

Whiticar, M. J., 1996. Stable isotope geochemistry of coals, humic kerogens and related natural gases. Int. J. Coal Geol. 32, 191–215.

Whiticar, M.J., Faber, E., Schoell, M., 1986. Biogenic methane formation in marine and freshwater environments: CO_2 reduction vs. acetate fermentation—isotope evidence. Geochim. Cosmochim. Acta 50, 693–709.

Xiao, D., Peng, S., Wang, B., Yan, X., 2013. Anthracite bio-degradation by methanogenic consortia in Qinshui basin. Int. J. Coal Geol. 116, 46–52.

Yoshinaga, M. Y., Holler, T., Goldhammer, T., Wegener, G., Pohlman, J.W., Brunner, B., Kuypers, M.M., Hinrichs, K.U., Elvert, M., 2014. Carbon isotope equilibration during sulphate-limited anaerobic oxidation of methane. Nat. Geosci. 7, 190–194.

Zhang, J., Liang, Y., Pandey, R., Harpalani, S., 2015. Characterizing microbial communities dedicated for conversion of coal to methane in situ and ex situ. Int. J. Coal Geol. 146, 145–154.

Zhou, Z., Ballentine, C.J., Kipfer, R., Schoell, M., Thibodeaux, S., 2005. Noble gas tracing of groundwater/coalbed methane interaction in the San Juan Basin, USA. Geochim. Cosmochim. Acta 69, 5413–5428.

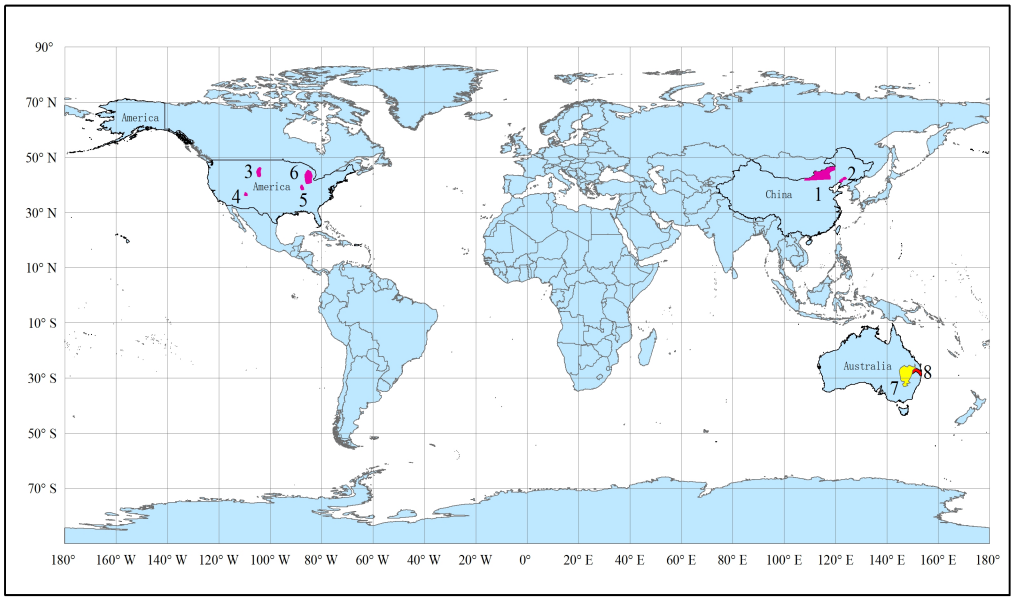

Fig. 1. Locations of basins in the study. (1) Erlian Basin, China. (2) Fuxin Basin, China. (3) Powder River Basin, USA. (4) San Juan Basin, USA. (5) Illinois Basin, USA. (6) Michigan Basin, USA. (7) Surat Basin, Australia. (8) Clarence-Moreton Basin, Australia.

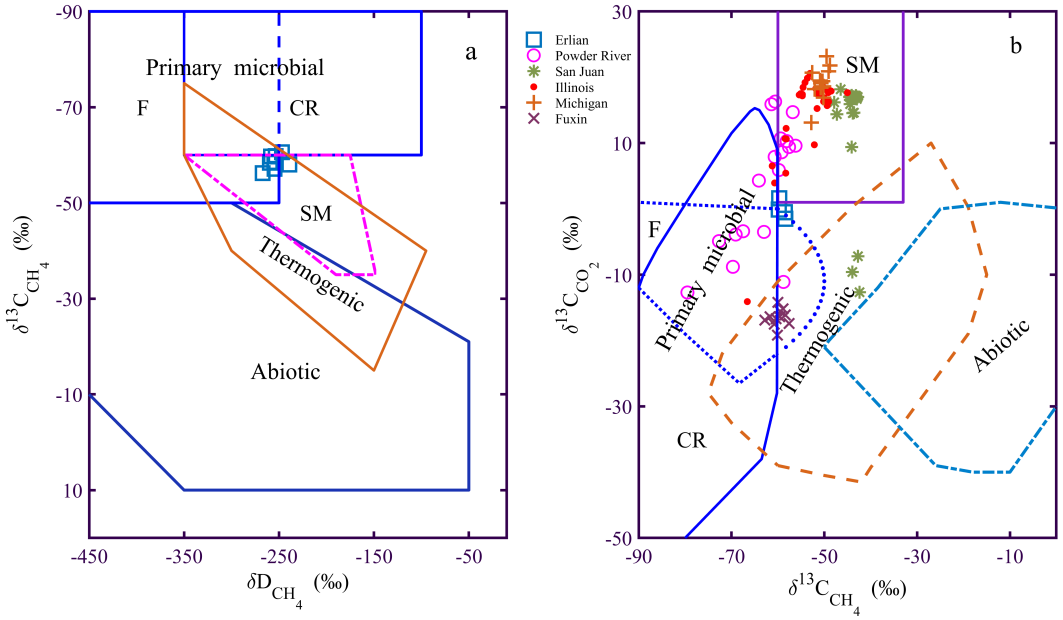

686

687 **Fig. 2. (a)** Genetic diagram of $\delta^{13}C_{CH4}$ vs. δD_{CH4} for CBG samples from the Erlian Basin (after
688 Milkov and Etiope, 2018). **(b)** Genetic diagram of $\delta^{13}C_{CO2}$ vs. $\delta^{13}C_{CH4}$ for CBG and SG samples
689 from various basins (after Milkov and Etiope, 2018). The two diagrams show that most of gas
690 samples are microbial in origins. The exception includes some samples from the San Juan
691 Basin. F: methyl-type fermentation; CR: CO_2 reduction; SM: secondary microbial. Data from
692 the Fuxin, the Powder River, the San Juan, the Illinois, and the Michigan Basins are from
693 literature (Bates et al., 2011; Chen et al., 2023; Martini et al., 1998; Schlegel et al., 2011; Zhou
694 et al., 2005) (See Supplementary Material). The new samples are from the Erlian Basin.

695

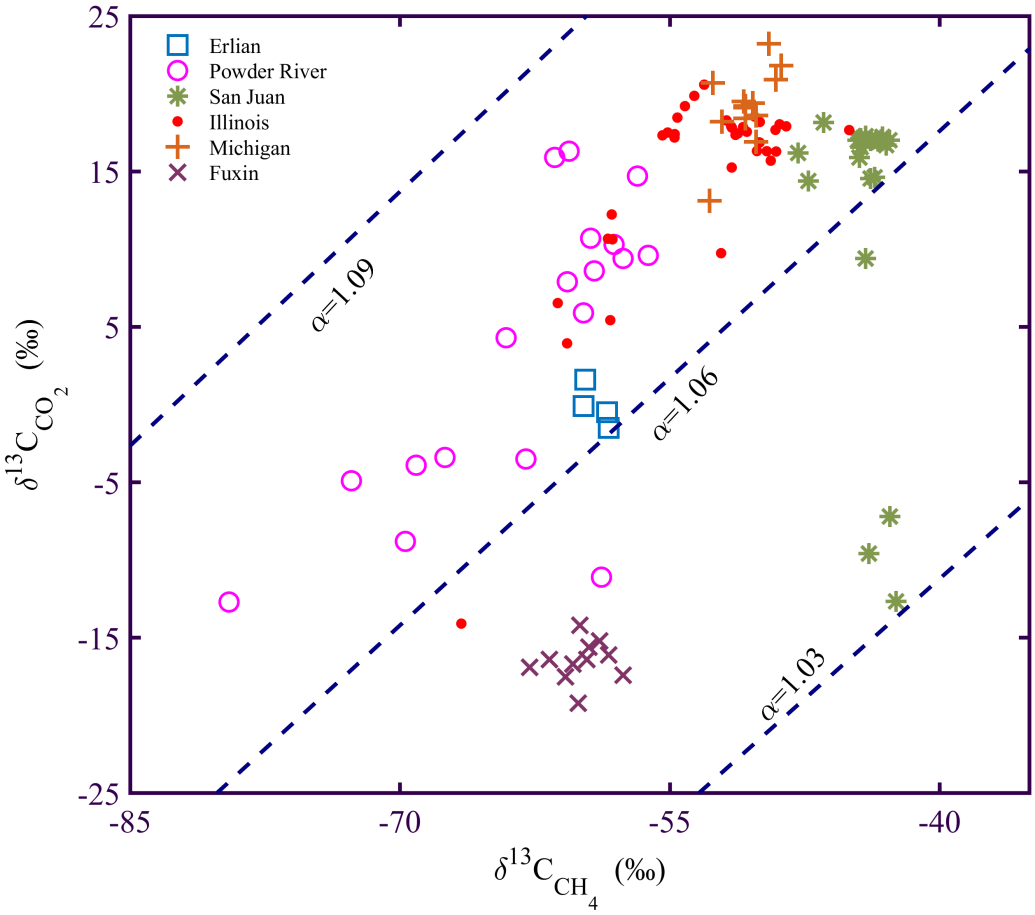

696

697 **Fig. 3.** Plot of $\delta^{13}C_{CH4}$ vs. $\delta^{13}C_{CO2}$ for CBG and SG samples from various basins. In general,
698 $\alpha_{CO2\text{-}CH4}$ values for CO_2 reduction and methyl-type fermentation range from 1.06 to 1.09, and
699 1.03 to 1.06, respectively. The distribution characteristics of data suggest that CO_2 reduction is
700 the dominant methanogenesis pathway in most gas samples. Data from the Fuxin, the Powder
701 River, the San Juan, the Illinois, and the Michigan Basins are from literature (Bates et al., 2011;
702 Chen et al., 2023; Martini et al., 1998; Schlegel et al., 2011; Zhou et al., 2005) (See
703 Supplementary Material). The samples from the Erlian Basin are new.

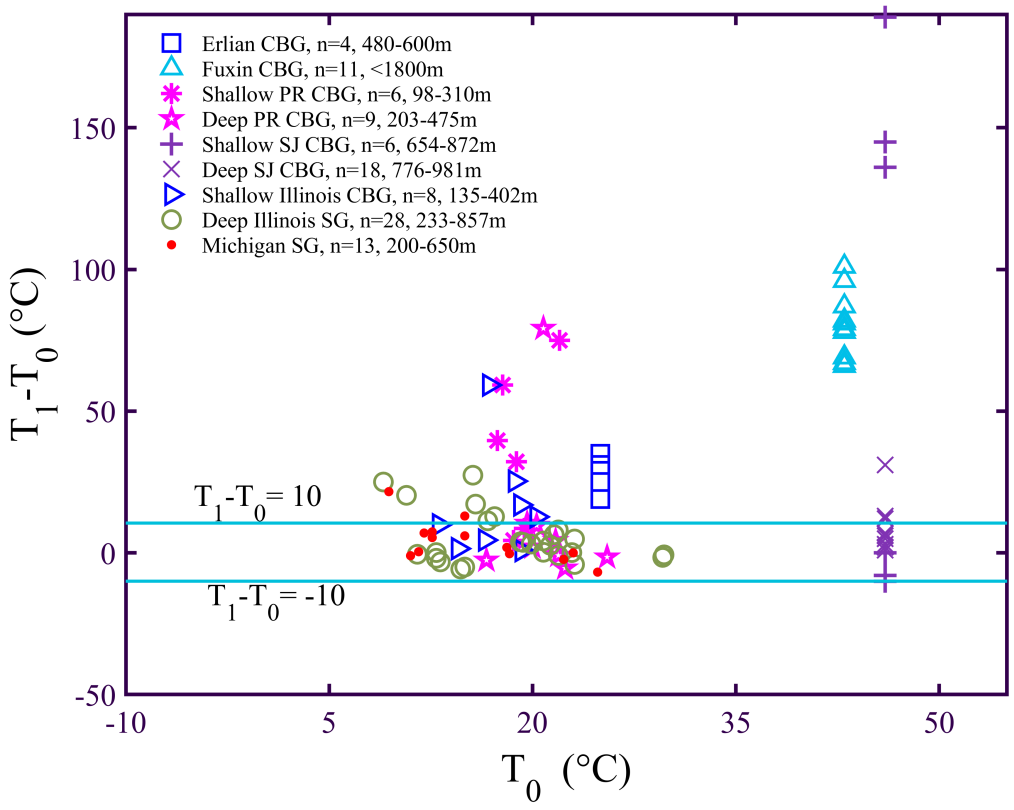

704

705 **Fig. 4.** Comparation of the calculated equilibrium temperature T_1 and the reservoir temperature

706 T_0 in various basins. T_1 is equilibrium temperature calculated by using $\delta^{13}C$ values of CH_4-CO_2.

707 Horizontal lines denote the threshold of ±10°C for T_2-T_0. In the samples from the Erlian and the

708 Fuxin Basins, CH_4-CO_2 is not in carbon isotopic equilibrium. For most samples from the deep

709 coalbeds of the Powder River (PR) Basin, CH_4-CO_2 is close to carbon isotopic equilibrium.

710 However, CH_4-CO_2 is in disequilibrium in most samples from shallow coalbeds. In the San Juan

711 (SJ) Basin, CH_4-CO_2 is close to carbon isotopic equilibrium for samples with deep burial depths,

712 however, CH_4-CO_2 is in disequilibrium for half of shallow samples. For most SG samples from

713 the deep shales of the Illinois Basin, CH_4-CO_2 is close to carbon isotopic equilibrium. For half of

714 samples from the shallow coalbeds in the basin, CH_4-CO_2 is in disequilibrium. In the Michigan

715 Basin, CH_4-CO_2 is close to carbon isotopic equilibrium in most samples.

716

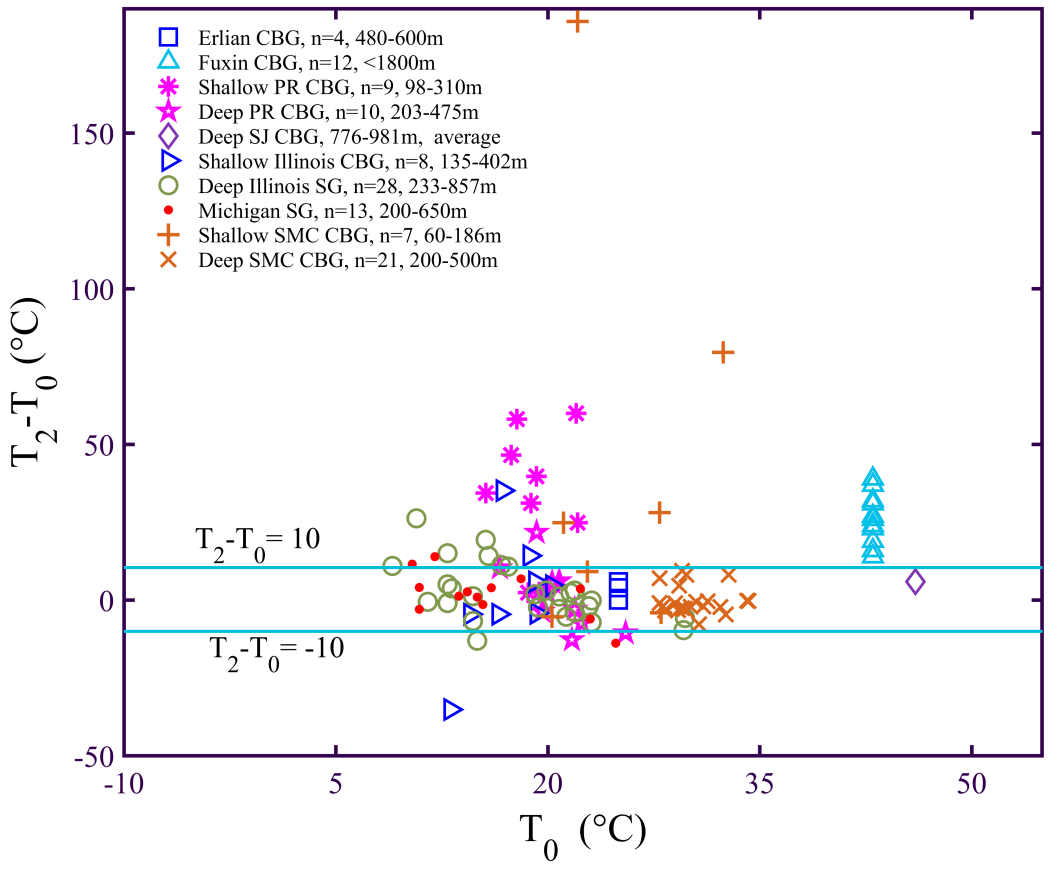

717

718 **Fig. 5.** Comparation of the calculated equilibrium temperature T_2 and the reservoir temperature
719 T_0 in various basins. T_2 is equilibrium temperature calculated by using $\delta^{13}C$ values of CH_4-
720 HCO_3^-. Horizontal lines denote the threshold of ±10°C for T_2-T_0. In the Erlian Basin samples,
721 CH_4-HCO_3^- is close to carbon isotopic equilibrium. In the Fuxin Basin samples, CH_4-HCO_3^- is in
722 carbon isotopic disequilibrium. For most samples from the deep coalbeds of the Powder River
723 (PR) Basin, CH_4-HCO_3^- is close to carbon isotopic equilibrium. However, CH_4-HCO_3^- is in
724 disequilibrium in most shallow samples. In the deep CBG reservoirs in the San Juan (SJ) Basin,
725 CH_4-HCO_3^- is close to carbon isotopic equilibrium. For most samples from the deep shales of the
726 Illinois Basin, CH_4-HCO_3^- is close to carbon isotopic equilibrium. For some samples from the
727 shallow coalbeds in the basin, CH_4-HCO_3^- is in disequilibrium. In the Michigan Basin samples,

728 CH_4-HCO_3^- is close to carbon isotopic equilibrium. In the Surat/Clarence-Moreton (SCM) Basin,
729 CH_4-HCO_3^- is close to carbon isotopic equilibrium for samples from deep coalbeds, however, it
730 is in disequilibrium for most samples from shallow coalbeds.
731

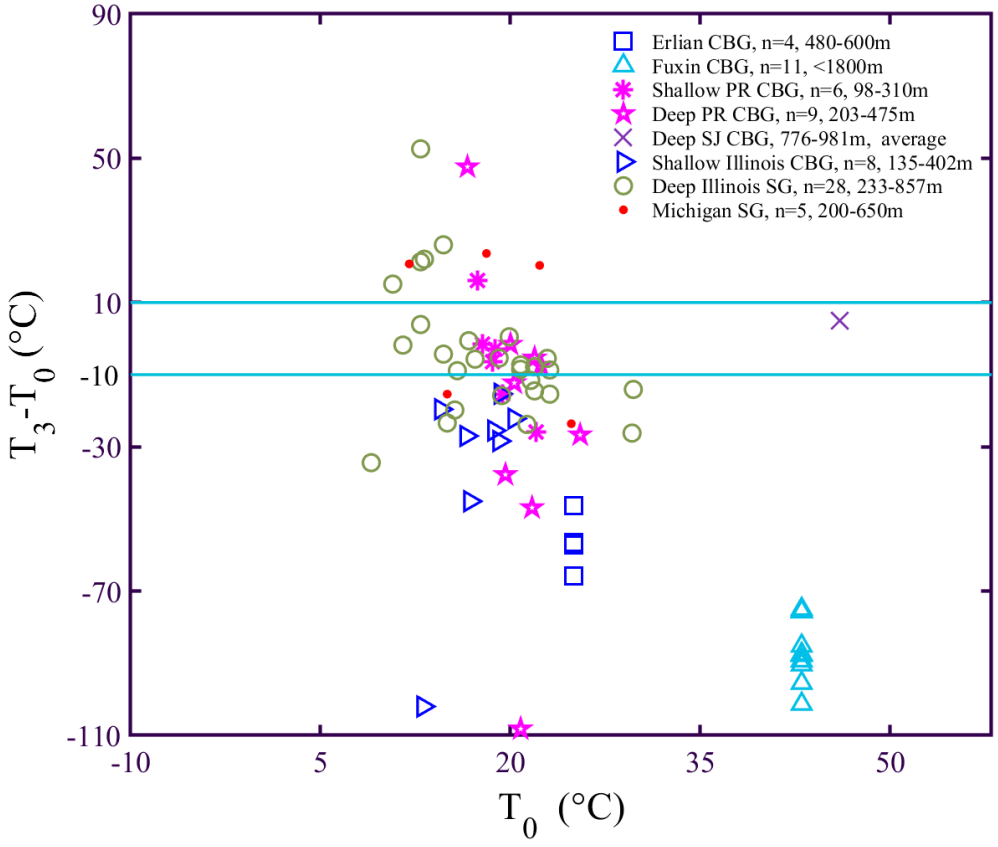

732

733 **Fig. 6.** Comparation of the calculated equilibrium temperature T_3 and the reservoir temperature

734 T_0 in various basins. T_3 is equilibrium temperature calculated by using $\delta^{13}C$ values of CO_2-

735 HCO_3^-. Horizontal lines denote the threshold of ±10°C for T_3-T_0. It indicates that CO_2-HCO_3^- is

736 in carbon isotope disequilibrium in most of samples.

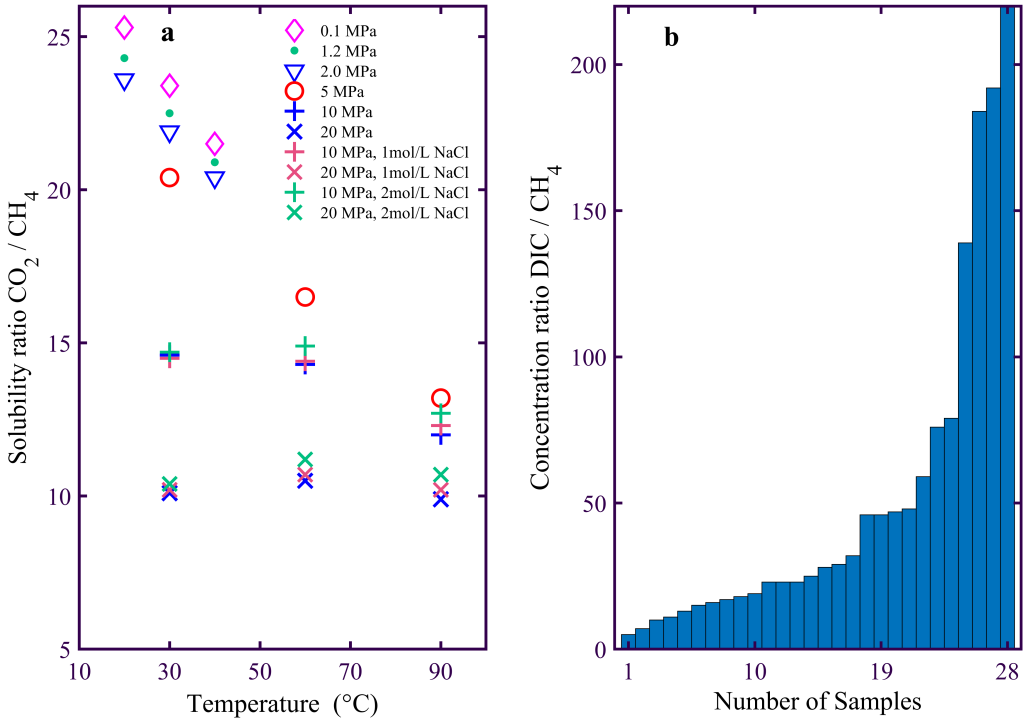

737

738 **Fig. 7.** Comparison of CO_2 and CH_4 dissolution effects. (a) The solubility ratio of CO_2/CH_4

739 under certain temperature, pressure and salinity conditions. The date are from Duan et al. (1992),

740 Sun, (2015), Diamond and Akinfiev, (2003), and Akinfiev and Diamond, (2010). (b) The

741 concentration ratio of DIC and dissolved CH_4 in coalbed water from the Surat and the Clarence-

742 Moreton Basins. The date are from Owen et al. (2016).

743

744 **Table 1.**

745 Molecular and isotopic compositions of CBG and coalbed water samples from the Erlian Basin*

Sample	Molecular composition (%)				Isotopic composition (‰)					$\Delta^{13}C_{CH4(aq)-CH4}$	$\alpha_{CO2-CH4}$
	CH_4	CO_2	N_2	Ar	$\delta^{13}C_{CH4}$	δD_{CH4}	$\delta^{13}C_{CO2}$	$\delta^{13}C_{CH4(aq)}$	$\delta^{13}C_{DIC}$		
J-1	96.5	3.5	0.0	0.02	-59.8	-253.5	-0.1	-56.1	+15.6	3.7	1.063
J-2	94.6	3.9	1.5	0.02	-58.5	-254.9	-0.5	-56.9	+15.1	1.6	1.062
J-3	96.8	3.2	0.0	0.02	-59.7	-258.5	+1.6	-56.2	+15.6	3.5	1.065
J-4	--	--	--	--	-58.4	-259.7	-1.5	-56.9	+15.7	1.5	1.059
J5-1	--	--	--	--	-56.2	-267.2	--	--	--	--	--
J5-2	--	--	--	--	-58.0	-239.2	--	--	--	--	--
J5-3	--	--	--	--	-60.6	-246.9	--	--	--	--	--
J5-4	--	--	--	--	-57.1	-254.7	--	--	--	--	--

746 * Samples J-1 to J-4 are from different CBG production wells, J5-1 to J5-4 are desorbed gas samples from a coal
747 core; $\delta^{13}C_{CH4(aq)}$ denotes dissolved methane $\delta^{13}C_{CH4}$; $\Delta^{13}C_{CH4(aq)-CH4} = \delta^{13}C_{CH4\ aq} - \delta^{13}C_{CH4}$; $\alpha_{CO2-CH4} = (\delta^{13}C_{CO2}$
748 $+1000)/(\delta^{13}C_{CH4}+1000)$; "--" denotes that data is not measured.
749

Table 2.

Summary of measured and calculated temperatures for all samples from various basins

Basin	Type	Stratum	Depth (m)	*Temperature (°C)						
				T_0	T_1	T_2	T_3	T_1-T_0	T_2-T_0	T_3-T_0
Erlian	CBG	LC	480-600	25	44~60	25~31	-41~-21	19~35	0~6	-66~-46
Fuxin	CBG	LC	<1800	38~48	109~144	57~82	-58~-32	66~101	14~39	-102~-75
PR	CBG	Tertiary	98-310	15.6~22.1	23~97	21~82	-4~34	4~75	2~60	-26~17
			203-475	16.6~25.5	14~100	9~41	-87~64	-5~79	-13~22	-108~48
SCM	CBG	MT	60-186	20.3~32.4	--	18~208	--	--	-5~186	--
			200-500	27.9~34.2	--	23~41	--	--	-8~10	--
SJ	CBG	UC	654-872	46	36~235	--	--	-10~189	--	--
			#776-981	46	47~77	52	--	1~31	6	--
Illinois	CBG	P	135-402	13.1~20.3	16~76	-22~52	-89~4	1~59	-35~35	-102~-15
	SG	UD	233-857	9.0~29.7	9~34	2~37	-25~66	-6~27	-13~26	-34~53
Michigan	SG	UD	200-650	9.4~24.8	10~31	8~26	0-43	-7~22	-14~14	-24~24

PR: Powder River; SCM: Surat/Clarence-Moreton; SJ: San Juan. LC: Lower Cretaceous; UC: Upper Cretaceous; MT: Middle Triassic; P: Pennsylvanian; UD: Upper Devonian. "--" denote that the data is not provided.

* T_0 denotes measured reservoir temperature. T_1, T_2 and T_3 denote calculated temperatures by using $\delta^{13}C$ values of CH_4-CO_2, CH_4-HCO_3^-, and CO_2-HCO_3^-, respectively.

For samples with depths of 776-981m, the average values of $\delta^{13}C_{DIC}$ and $\delta^{13}C_{CH4}$ are used to calculate T_2, because only the average $\delta^{13}C_{DIC}$ value of 23‰ is reported (Scott et al., 1994).

Table 3.

Calculated percentage of CO_2 in total CH_4 and CO_2 and percentage of dissolved CO_2 in total CO_2 in various microbial CBG basins.

Basin	Average value (‰)				$CO_2/(CO_2+CH_4)$ (%)	$^{\#}X_{CO2}/(X_{CO2}+X_{CH4})$ (%)		CO_2 (%)	
	$\delta^{13}C_{CH4}$	$\delta^{13}C_{CO2}$	$\delta^{13}C_{DIC}$	$^{*}\delta^{13}C_{coal}$		Lower	Upper	Gaseous	Dissolved
Erlian	-59.1±0.7	--	15.5±0.2	-22.0	4±1	50	-	2	98
PR	-58.5±1.5	9.6±2.4	--	-25.7	5±5	--	48	--	--
	-58.6±1.4	--	18.8±2.2	-25.7	8±9	43	--	11	89
SCM	-55.3±2.7	--	18.0±4.1	-24.5	--	42	--	--	--
Illinois	-58.8±1.0	--	20.3±3.3	-25.1	1±0	43	--	1	99
SJ	-43.7±0.6	16.9±0.3	23.0	25.7	15±2	27	30	47	53

PR: Powder River; SCM: Surat/Clarence-Moreton; SJ: San Juan. "--" denotes the data is not measured or calculated.

* The $\delta^{13}C_{coal}$ values of five coal samples from the Erlian Basin are -22.6, -21.8, -22.0, -21.4, and -21.9‰; The $\delta^{13}C_{coal}$ value of the Illinois Basin is from Rahman et al. (2017); The $\delta^{13}C_{coal}$ values from other basins are from Suto and Kawashima (2016).

$^{\#}$ Lower/Upper: calculated lower/upper limit of percentage of CO_2 in total CH_4 and CO_2.